

Pattern Formation in Turing Systems on Domains with Exponentially Growing Structures

Gregory Toole · Monica K. Hurdal

Received: 27 August 2012 / Revised: 16 May 2013 / Published online: 2 April 2014
© Springer Science+Business Media New York 2014

Abstract Turing reaction–diffusion systems have been used to model pattern formation in several areas of developmental biology. Previous biomathematical Turing system models employed static domains which failed to incorporate the growth that inherently occurs as an organism develops. To address this shortcoming, we incorporate an exponentially growing domain into a Turing system, allowing one to more realistically model biological pattern formation. This Turing system can generate patterns on an exponentially growing domain in any of the eleven coordinate systems in which the Helmholtz equation is separable, making the system incredibly flexible and giving one the capability to mathematically model pattern formation on a geometrically diverse group of domains. Linear stability analysis is employed to generate mathematical conditions which ensure such a system can generate patterns. We apply the exponentially growing Turing system to a prolate spheroidal domain and conduct numerical simulations to investigate the system’s pattern-generating behavior. We find that the addition of growth to a Turing system causes a significant change in the pattern-generating behavior of the system. While a static domain Turing system converges to a final pattern, an exponentially growing domain Turing system produces transient patterns that continually evolve and increase in complexity over time.

Keywords Turing system · Turing pattern · Reaction–diffusion system · Growing domain · Pattern formation

Mathematics Subject Classification 35B36 · 35K57 · 92C15

G. Toole
Polk State College, Winter Haven, FL 33881, USA

G. Toole · M. K. Hurdal (✉)
Department of Mathematics, Florida State University,
Tallahassee, FL 32306-4510, USA
e-mail: mhurdal@math.fsu.edu

1 Introduction

In 1952, A.M. Turing developed a system of reaction–diffusion equations to describe formation of chemical gradient patterns on the developing embryo [15]. Since Turing’s classic paper, research has been conducted on applying these “Turing systems” to model pattern formation associated with developmental biology phenomena such as leopard spots, zebra stripes, and more [11]. Recently, evidence has been found in mice to support the plausibility of using a Turing system to model biological pattern formation [13].

Let $u(\mathbf{X}, t)$ and $v(\mathbf{X}, t)$ be the concentrations at position \mathbf{X} and time t of an activator morphogen and an inhibitor morphogen, respectively, on a static domain. Consider the reaction–diffusion system

$$\left. \begin{aligned} \frac{\partial u}{\partial t} &= d_u \nabla^2 u + f(u, v), \\ \frac{\partial v}{\partial t} &= d_v \nabla^2 v + g(u, v), \end{aligned} \right\} \quad (1)$$

where $f(u, v)$, $g(u, v)$ are the reaction kinetics and $d_u, d_v > 0$ are the diffusion coefficients for the activator and inhibitor, respectively. System 1 is called a Turing system and is capable of generating spatially inhomogeneous patterns when it possesses a spatially uniform steady state (u_0, v_0) which is linearly stable in the absence of diffusion but unstable in the presence of diffusion; these properties are often referred to as the Turing criteria. Turing systems require that the diffusion coefficient of the inhibitor be greater than that of the activator, so that $d_u < d_v$ [11]. The resulting “short range activation, long range inhibition” [6] is observed in numerous biological phenomena, such as organogenesis in transplants [6] and hair follicle development in mice [13].

Previous biomathematical Turing system models utilized static domains; that is, the domain upon which the Turing system produced patterns did not change in size. A growing domain Turing system may be a more realistic way to model pattern formation in biological phenomena since it incorporates the growth that inherently occurs as an organism develops. In this paper, we extend previous static domain Turing system research [11, 14] by investigating the role of an exponentially growing domain in a Turing system. Mathematical conditions whose satisfaction ensures the system will exhibit the characteristic pattern-generating Turing behavior will be derived. Finally, numerical results will be implemented with BVM kinetics [3].

2 Growing Domain Turing System Framework

Plaza et al. [12] constructed a general framework in which domain growth can be incorporated into a Turing reaction–diffusion system. Let $S_t \subset \mathbb{R}^3$ be a two-dimensional regular growing surface with position vector $\mathbf{X} = \mathbf{X}(\zeta, \eta, t)$ upon which two chemical substances $u = u(\mathbf{X}, t)$ and $v = v(\mathbf{X}, t)$ are reacting and diffusing. If D_u, D_v are the diffusion coefficients of u, v , respectively, then after nondimensionalization System 1 becomes

$$\left. \begin{aligned} u_t &= D \Delta_s u - \partial_t (\ln(h_1 h_2)) u + \omega f(u, v), \\ v_t &= \Delta_s v - \partial_t (\ln(h_1 h_2)) v + \omega g(u, v), \end{aligned} \right\} \quad (2)$$

where

$$\Delta_s \phi = \frac{1}{h_1 h_2} \left[\left(\frac{h_2}{h_1} \phi_\zeta \right)_\zeta + \left(\frac{h_1}{h_2} \phi_\eta \right)_\eta \right] \tag{3}$$

is the Laplace–Beltrami operator on $S_t(\phi = u, v)$, $h_1 = |\mathbf{X}_\zeta|$, $h_2 = |\mathbf{X}_\eta|$, $D = D_u/D_v \in (0, 1)$, $\omega > 0$ is the domain scale parameter, and f, g are the dimensionless reaction kinetics. The term $-\partial_t (\ln(h_1 h_2)) \phi$ in each equation of System 2 models dilution of the morphogen concentration due to the growth of the domain [12]. The domain scale parameter ω is used to control the strength of the reaction terms versus that of the diffusion and dilution terms. Reaction terms create peaks of morphogen concentration, while diffusion and dilution terms smooth out peaks of concentration. The interplay between peak creation and peak smoothing results in pattern formation. System 2 provides a general framework for a Turing reaction–diffusion system on a growing domain S_t . The growth of S_t is isotropic with growth function $\rho(t)$ when $\mathbf{X}(\zeta, \eta, t) = \rho(t) \mathbf{X}_0(\zeta, \eta)$ [12].

For this investigation, we let S_t be an exponentially growing domain in one of the eleven coordinate systems in which the Helmholtz equation is separable [18]. We define the position vector \mathbf{X} on S_t as

$$\mathbf{X}(\zeta, \eta, t) = \rho(t) \begin{pmatrix} x_0(\zeta, \eta) \\ y_0(\zeta, \eta) \\ z_0(\zeta, \eta) \end{pmatrix} = \rho(t) \mathbf{X}_0(\zeta, \eta),$$

where $t \geq 0$, $\rho(t) = e^{Rt}$ is the growth function with growth rate $R > 0$, and \mathbf{X}_0 parameterizes the domain at $t = 0$. As discussed above, defining \mathbf{X} in this way gives isotropic domain growth. It then follows that

$$h_1 = |\mathbf{X}_\zeta| = \rho(t) |\partial_\zeta \mathbf{X}_0|$$

and

$$h_2 = |\mathbf{X}_\eta| = \rho(t) |\partial_\eta \mathbf{X}_0|,$$

so the dilution term becomes

$$\begin{aligned} -\partial_t (\ln(h_1 h_2)) \phi &= -\frac{\partial}{\partial t} (\ln(\rho^2 |\partial_\zeta \mathbf{X}_0| |\partial_\eta \mathbf{X}_0|)) \phi \\ &= -2 \frac{\dot{\rho}}{\rho} \phi, \end{aligned}$$

where $\phi = u, v$ and $(\dot{\cdot})$ denotes the time derivative $\frac{\partial}{\partial t}(\cdot)$. Since $\rho(t) = e^{Rt}$, it follows that

$$-\partial_t (\ln(h_1 h_2)) \phi = -2R\phi.$$

Thus, a Turing system on an exponentially growing domain takes the form

$$\left. \begin{aligned} u_t &= D \Delta_s u - 2Ru + \omega f(u, v), \\ v_t &= \Delta_s v - 2Rv + \omega g(u, v), \end{aligned} \right\} \tag{4}$$

where $u = u(\zeta, \eta, t)$, $v = v(\zeta, \eta, t)$. Note that setting $R = 0$ transforms System 4 into a nondimensional static domain reaction–diffusion system [11]; this will be discussed in more detail in Sect. 6.

3 Deriving Turing Conditions: Linear Stability Analysis

It is desirable to determine mathematical conditions that System 4 must satisfy in order to satisfy the two Turing criteria and hence be able to generate Turing patterns. These mathematical conditions shall hereupon be referred to as Turing conditions. One should note the difference between the Turing criteria described in Sect. 1, which describe the system’s behavior in the presence and absence of diffusion, and Turing conditions, which are mathematical equations whose satisfaction implies compliance with the Turing criteria. Linear stability analysis has been widely used to derive Turing conditions for static domain Turing systems [11, 15]. For this paper, we will apply linear stability analysis to the growing domain System 4 following the methods of [7].

3.1 First Turing Criterion: Linear Stability in the Absence of Diffusion

Notice that the Laplace–Beltrami operator in Eq. 3 can be rewritten as

$$\Delta_s \phi = \frac{1}{\rho^2} \Delta_{\dagger} \phi,$$

where

$$\Delta_{\dagger} \phi = \frac{1}{|\partial_{\zeta} \mathbf{X}_0| |\partial_{\eta} \mathbf{X}_0|} \left[\left(\frac{|\partial_{\eta} \mathbf{X}_0|}{|\partial_{\zeta} \mathbf{X}_0|} \phi_{\zeta} \right)_{\zeta} + \left(\frac{|\partial_{\zeta} \mathbf{X}_0|}{|\partial_{\eta} \mathbf{X}_0|} \phi_{\eta} \right)_{\eta} \right].$$

This allows System 4 to be rewritten as

$$\left. \begin{aligned} u_t &= \frac{D}{\rho^2} \Delta_{\dagger} u - 2Ru + \omega f(u, v), \\ v_t &= \frac{1}{\rho^2} \Delta_{\dagger} v - 2Rv + \omega g(u, v). \end{aligned} \right\} \tag{5}$$

In the absence of diffusion, System 5 becomes

$$\left. \begin{aligned} u_t &= -2Ru + \omega f(u, v), \\ v_t &= -2Rv + \omega g(u, v). \end{aligned} \right\} \tag{6}$$

Assume System 5 has a spatially uniform steady state (u_0, v_0) which remains a steady state in the absence of diffusion; that is, (u_0, v_0) is the solution to

$$\left. \begin{aligned} 0 &= -2Ru_0 + \omega f(u_0, v_0), \\ 0 &= -2Rv_0 + \omega g(u_0, v_0). \end{aligned} \right\} \tag{7}$$

Define

$$\mathbf{w}(t) = \begin{pmatrix} u(t) - u_0 \\ v(t) - v_0 \end{pmatrix} = \begin{pmatrix} \epsilon_u \\ \epsilon_v \end{pmatrix} \tag{8}$$

to be a perturbation from the steady state (u_0, v_0) , where $0 < |\epsilon_u|, |\epsilon_v| \ll 1$. Using Eq. 8, System 6 can be rewritten as

$$\begin{aligned} \mathbf{w}_t &= \begin{pmatrix} u_t \\ v_t \end{pmatrix} = \begin{pmatrix} -2Ru + \omega f(u, v) \\ -2Rv + \omega g(u, v) \end{pmatrix} \\ &= \begin{pmatrix} -2R(u_0 + \epsilon_u) + \omega f(u_0 + \epsilon_u, v_0 + \epsilon_v) \\ -2R(v_0 + \epsilon_v) + \omega g(u_0 + \epsilon_u, v_0 + \epsilon_v) \end{pmatrix}. \end{aligned} \tag{9}$$

System 6 can be analyzed by linearizing the nonlinear kinetics functions f and g about the steady state (u_0, v_0) . A Taylor expansion of u_t from Eq. 9 about (u_0, v_0) gives

$$u_t = -2Ru_0 + \omega f(u_0, v_0) + \epsilon_u \frac{\partial}{\partial u} (-2Ru + \omega f(u, v)) |_{(u_0, v_0)} + \epsilon_v \frac{\partial}{\partial v} (-2Ru + \omega f(u, v)) |_{(u_0, v_0)} + O(\epsilon^2). \tag{10}$$

Since (u_0, v_0) is a steady state of System 6, Eq. 10 can be rewritten as

$$u_t \approx \epsilon_u (-2R + \omega f_u(u_0, v_0)) + \epsilon_v \omega f_v(u_0, v_0), \tag{11}$$

where $f_u = \frac{\partial f}{\partial u}$ and $f_v = \frac{\partial f}{\partial v}$. Similarly,

$$v_t \approx \epsilon_u \omega g_u(u_0, v_0) + \epsilon_v (-2R + \omega g_v(u_0, v_0)). \tag{12}$$

Equations 8–12 imply

$$\begin{aligned} u_t &\approx -2R\epsilon_u + \omega [\epsilon_u f_u(u_0, v_0) + \epsilon_v f_v(u_0, v_0)], \\ v_t &\approx -2R\epsilon_v + \omega [\epsilon_u g_u(u_0, v_0) + \epsilon_v g_v(u_0, v_0)], \end{aligned}$$

and

$$\mathbf{w}_t = -2R\mathbf{w} + \omega A\mathbf{w}, \tag{13}$$

where

$$A = \begin{pmatrix} f_u & f_v \\ g_u & g_v \end{pmatrix}_{(u_0, v_0)}. \tag{14}$$

Consider solutions to Eq. 13 of form $\mathbf{w}(t) = \mathbf{c}e^{\lambda t}$, where \mathbf{c} represents constants. Linear stability of (u_0, v_0) in the absence of diffusion implies $\mathbf{w} \rightarrow \mathbf{0}$ as $t \rightarrow \infty$, which occurs precisely when $Re \lambda < 0$. Substituting $\mathbf{w}(t) = \mathbf{c}e^{\lambda t}$ into Eq. 13 yields

$$\lambda \mathbf{c}e^{\lambda t} = \omega A \mathbf{c}e^{\lambda t} - 2R \mathbf{c}e^{\lambda t}. \tag{15}$$

Dividing Eq. 15 through by $e^{\lambda t}$ gives the eigenvalue equation

$$\begin{aligned} \lambda \mathbf{c} &= \omega A \mathbf{c} - 2R \mathbf{c}, \\ &= \tilde{A} \mathbf{c}, \end{aligned}$$

where

$$\tilde{A} = \omega A - 2RI = \begin{pmatrix} \omega f_u - 2R & \omega f_v \\ \omega g_u & \omega g_v - 2R \end{pmatrix}_{(u_0, v_0)}.$$

The characteristic equation of \tilde{A} ,

$$\det(\tilde{A} - \lambda I) = \begin{vmatrix} \omega f_u - 2R - \lambda & \omega f_v \\ \omega g_u & \omega g_v - 2R - \lambda \end{vmatrix} = 0, \tag{16}$$

implies that the eigenvalues λ of \tilde{A} satisfy the characteristic polynomial

$$\lambda^2 - \lambda \text{tr } \tilde{A} + \det \tilde{A} = 0, \tag{17}$$

where

$$\begin{aligned} \text{tr } \tilde{A} &= \omega(f_u + g_v) - 4R \quad \text{and} \\ \det \tilde{A} &= \omega^2(f_u g_v - f_v g_u) - 2R\omega(f_u + g_v) + 4R^2. \end{aligned}$$

Since Eq. 17 has solutions

$$\lambda_{1,2} = \frac{1}{2} \operatorname{tr} \tilde{A} \pm \frac{1}{2} \sqrt{(\operatorname{tr} \tilde{A})^2 - 4 \det \tilde{A}},$$

it then follows that $Re \lambda$ will always be negative when

$$\operatorname{tr} \tilde{A} < 0 \quad \text{and} \tag{18a}$$

$$\det \tilde{A} > 0, \tag{18b}$$

which are the two mathematical conditions required for System 4 to satisfy the first Turing criterion.

3.2 Second Turing Criterion: Diffusion-Driven Instability

System 5 can be linearized around the steady state (u_0, v_0) to yield

$$\mathbf{w}_t = D_M \Delta \dagger \mathbf{w} - 2R\mathbf{w} + \omega A\mathbf{w}, \tag{19}$$

where \mathbf{w} is the perturbation from the steady state (u_0, v_0) defined in Eq. 8 and

$$D_M = \frac{1}{\rho^2} \begin{pmatrix} D & 0 \\ 0 & 1 \end{pmatrix}.$$

Let the solutions \mathbf{w} to Eq. 19 be of form

$$\mathbf{w}(\mathbf{X}, t) = \sum_k c_k e^{\lambda t} \mathbf{Y}_k(\mathbf{X}), \tag{20}$$

where \mathbf{Y}_k are solutions to the Helmholtz equation on S_t (that is, they satisfy $\Delta \mathbf{Y}_k + k^2 \mathbf{Y}_k = 0$ on S_t) and c_k are the Fourier coefficients, which depend on the initial conditions. Substituting Eq. 20 into Eq. 19 implies

$$\sum_k c_k \lambda e^{\lambda t} \mathbf{Y}_k = D_M \sum_k c_k e^{\lambda t} \Delta \dagger \mathbf{Y}_k - 2R \sum_k c_k e^{\lambda t} \mathbf{Y}_k + \omega A \sum_k c_k e^{\lambda t} \mathbf{Y}_k,$$

which, after dividing through by $e^{\lambda t}$ can be rewritten as

$$\sum_k c_k (\lambda \mathbf{Y}_k - D_M \Delta \dagger \mathbf{Y}_k + 2R\mathbf{Y}_k - \omega A\mathbf{Y}_k) = 0. \tag{21}$$

The fact that \mathbf{Y}_k satisfy the Helmholtz equation allows Eq. 21 to be rewritten as

$$\sum_k c_k (\lambda \mathbf{Y}_k + D_M k^2 \mathbf{Y}_k + 2R\mathbf{Y}_k - \omega A\mathbf{Y}_k) = 0.$$

Since we desire nontrivial \mathbf{w} , it follows that

$$\lambda \mathbf{Y}_k + D_M k^2 \mathbf{Y}_k + 2R\mathbf{Y}_k - \omega A\mathbf{Y}_k = 0,$$

which can be rewritten in the form of an eigenvalue equation,

$$\lambda \mathbf{Y}_k = (-D_M k^2 - 2RI + \omega A) \mathbf{Y}_k,$$

leading to the characteristic equation

$$\det (\tilde{A} - D_M k^2 - \lambda I) = 0. \tag{22}$$

If we allow $k^2 = 0$, then Eq. 22 reduces to Eq. 16, which is exactly the first Turing criterion (no diffusion) problem. Thus, for diffusion-driven instability we consider only $k^2 > 0$.

When evaluated, the determinant in Eq. 22 can be rewritten as

$$\lambda^2 + \lambda \left[\frac{k^2}{\rho^2} (1 + D) - \text{tr } \tilde{A} \right] + h(k^2) = 0, \tag{23}$$

where

$$h(k^2) = \frac{D}{\rho^4} (k^2)^2 + \frac{k^2}{\rho^2} [2R(1 + D) - \omega(f_u + Dg_v)] + \det \tilde{A}.$$

Notice that $h(k^2)$ is a quadratic equation in k^2 and that its constant term equals $\det \tilde{A}$. Solving for λ yields

$$\begin{aligned} \lambda_{1,2} = & -\frac{1}{2} \left(\frac{k^2}{\rho^2} (1 + D) - \text{tr } \tilde{A} \right) \\ & \pm \frac{1}{2} \sqrt{\left(\frac{k^2}{\rho^2} (1 + D) - \text{tr } \tilde{A} \right)^2 - 4h(k^2)}. \end{aligned} \tag{24}$$

Diffusion-driven instability of steady state (u_0, v_0) occurs when $Re \lambda > 0$, which is satisfied when either

$$\frac{k^2}{\rho^2} (1 + D) - \text{tr } \tilde{A} < 0 \tag{25}$$

or

$$\begin{aligned} \lambda = & -\frac{1}{2} \left(\frac{k^2}{\rho^2} (1 + D) - \text{tr } \tilde{A} \right) \\ & + \frac{1}{2} \sqrt{\left(\frac{k^2}{\rho^2} (1 + D) - \text{tr } \tilde{A} \right)^2 - 4h(k^2)} \end{aligned} \tag{26}$$

and

$$h(k^2) < 0. \tag{27}$$

From Eq. 18a, $-\text{tr } \tilde{A} > 0$. Recall that $\rho^2, D, k^2 > 0$ which implies $\frac{k^2}{\rho^2} (1 + D) > 0$. It then follows that Eq. 25 cannot be satisfied if the first Turing criterion is to be satisfied as well. Thus, in order to satisfy the second Turing criterion, Eqs. 26 and 27 must hold. A necessary condition to satisfy $h(k^2) < 0$ is

$$2R(1 + D) - \omega(f_u + Dg_v) < 0 \tag{28}$$

since $\frac{D}{\rho^4} (k^2)^2 > 0$, $\frac{k^2}{\rho^2} > 0$, and $\det \tilde{A} > 0$ (by Eq. 18b). Equation 28 is the first mathematical condition that must hold to achieve diffusion-driven instability, and the third mathematical condition overall for System 4 to be a Turing system. Notice that this is a necessary but not sufficient condition, as the positive square root coefficient of Eq. 24 must be selected. Another reason that Eq. 28 is necessary but not sufficient for $h(k^2) < 0$ is that $\frac{k^2}{\rho^2} [2R(1 + D) - \omega(f_u + Dg_v)]$ must not only be negative but also greater in magnitude than $\frac{D}{\rho^4} (k^2)^2 + \det \tilde{A}$. Also notice that setting $D = 1$ in Eq. 28 gives

$$4R - \omega(f_u + g_v) < 0,$$

which directly contradicts Eq. 18a. Thus, for System 4 to be a Turing system, D must satisfy $D \neq 1$, which is also true of static domain Turing systems [11].

In order to ensure $h(k^2) < 0$ and thus $Re \lambda > 0$, we derive a fourth Turing condition. For $h(k^2) < 0$ to be satisfied, it must be that $h_{\min} = \min [h(k^2)] < 0$, since $h(k^2)$ is an upward-opening parabola. To this end, differentiate $h(k^2)$ with respect to k^2 and set the derivative to zero to find that h_{\min} occurs at

$$k^2 = k_{\min}^2 = -\frac{\rho^2}{2D} [2R(1 + D) - \omega(f_u + Dg_v)],$$

so

$$\begin{aligned} h_{\min} = h(k_{\min}^2) = & R^2 \left[4 - \frac{(1 + D)^2}{D} \right] \\ & + R\omega \left[\frac{1}{D} (1 + D) (f_u + Dg_v) - 2(f_u + g_v) \right] \\ & + \omega^2 \left[(f_u g_v - f_v g_u) - \frac{1}{4D} (f_u + Dg_v)^2 \right]. \end{aligned}$$

Hence, to satisfy $h(k^2) < 0$, it must be that

$$\begin{aligned} R^2 \left[4 - \frac{(1 + D)^2}{D} \right] + R\omega \left[\frac{1}{D} (1 + D) (f_u + Dg_v) - 2(f_u + g_v) \right] \\ + \omega^2 (f_u g_v - f_v g_u) < \frac{\omega^2}{4D} (f_u + Dg_v)^2, \end{aligned} \tag{29}$$

which is the second mathematical condition required for diffusion-driven instability and the fourth and final mathematical condition required for System 4 to be a Turing system.

3.3 Summary of Turing System Conditions on an Exponentially Growing Domain

The four mathematical conditions required for the exponentially growing domain reaction–diffusion System 4 to be a Turing system are:

$$\left. \begin{aligned} \omega(f_u + g_v) - 4R &< 0, \\ \omega^2(f_u g_v - f_v g_u) - 2R\omega(f_u + g_v) + 4R^2 &> 0, \\ 2R(1 + D) - \omega(f_u + Dg_v) &< 0, \\ R^2 \left[4 - \frac{(1 + D)^2}{D} \right] + \omega^2(f_u g_v - f_v g_u) \\ + R\omega \left[\frac{1}{D} (1 + D) (f_u + Dg_v) - 2(f_u + g_v) \right] &< \frac{\omega^2}{4D} (f_u + Dg_v)^2, \end{aligned} \right\} \tag{30}$$

where the first two conditions give linear stability in the absence of diffusion and the second two conditions give diffusion-driven instability. Recall that the third condition is necessary but not sufficient, as it requires

$$\begin{aligned} \lambda = & -\frac{1}{2} \left(\frac{k^2}{\rho^2} (1 + D) - \omega(f_u + g_v) + 4R \right) \\ & + \frac{1}{2} \sqrt{\left(\frac{k^2}{\rho^2} (1 + D) - \omega(f_u + g_v) + 4R \right)^2 - 4h(k^2)} \end{aligned}$$

and

$$h(k^2) < 0.$$

4 Exponentially Growing Domain Turing System with BVM Kinetics

The phenomenological BVM kinetics [3] have been used to study pattern formation in a number of areas of biology, including fish pigmentation [2,3] and sea urchin podia development [1]. The static domain nondimensional Turing reaction–diffusion system with nondimensional BVM kinetics [1, 16] is given by

$$\left. \begin{aligned} \frac{\partial u}{\partial t} &= D\nabla^2 u + \omega(u + av - Cuv - uv^2), \\ \frac{\partial v}{\partial t} &= \nabla^2 v + \omega(bv + hu + Cuv + uv^2), \end{aligned} \right\} \tag{31}$$

where $D = D_u/D_v \in (0, 1)$ is the ratio of diffusion coefficients, $\omega > 0$ is the domain scale parameter, and a, b, C, h are kinetics parameters. The parameter C controls the relative strength of cubic and quadratic interactions; for large C quadratic interactions dominate, while for small C cubic interactions dominate [8]. On a static domain, the nondimensional BVM system tends to produce spotted patterns when quadratic interactions are present ($C > 0$) and striped patterns when quadratic interactions are nonexistent or very minimal ($C = 0$ or C near zero) [3,4].

We insert nondimensional BVM kinetics into our exponentially growing domain System 4, yielding

$$\left. \begin{aligned} u_t &= D\Delta_s u - 2Ru + \omega(u + av - Cuv - uv^2), \\ v_t &= \Delta_s v - 2Rv + \omega(bv + hu + Cuv + uv^2). \end{aligned} \right\} \tag{32}$$

4.1 Ensuring the Origin is the Only Steady State

Traditional use of BVM kinetics in static domain Turing systems sets parameter values so that $(0, 0)$ is the only spatially uniform steady state of the system. It is desirable to accomplish this for the exponentially growing domain System 32 as well. However, adding growth to a reaction–diffusion system adds the dilution term which must be considered when finding the steady state(s) of System 32. Recall that the steady state of any Turing system must remain a steady state in the absence of diffusion. A steady state $(u, v) = (u_0, v_0)$ of System 32 must then satisfy

$$0 = -2Ru_0 + \omega(u_0 + av_0 - Cu_0v_0 - u_0v_0^2), \tag{33a}$$

$$0 = -2Rv_0 + \omega(bv_0 + hu_0 + Cu_0v_0 + u_0v_0^2), \tag{33b}$$

from which it follows that

$$v_0 = \frac{-u_0(-2R + \omega + \omega h)}{-2R + \omega a + \omega b} \tag{34}$$

if $-2R + \omega a + \omega b \neq 0$. Requiring $-2R + \omega + \omega h = 0$, which implies

$$h = \frac{2R}{\omega} - 1, \tag{35}$$

ensures that $v_0 = 0$ is the only possible v coordinate of the steady state. Substituting $v_0 = 0$ into Eq. 33b yields

$$0 = \omega hu_0.$$

As $\omega > 0$, requiring $h \neq 0$ ensures that $u_0 = 0$.

In summary, in order for $(0, 0)$ to be the only steady state of System 32, it must be that

$$\left. \begin{aligned} -2R + \omega a + \omega b &\neq 0, \\ h = \frac{2R}{\omega} - 1 &\neq 0, \text{ and} \\ \omega &\neq 2R, \end{aligned} \right\} \tag{36}$$

where the third equation follows readily from the second.

4.2 Selecting Parameters

The numerous parameters of System 32 must have values that satisfy each of the following:

1. The Turing system diffusion coefficient requirement $0 < D_u < D_v$ (for nondimensional BVM kinetics, this means $0 < D < 1$),
2. The conditions required to make $(0, 0)$ the only steady state given by System 36, and
3. The four mathematical Turing conditions in 30.

It is important to note that ensuring D satisfies $D < 1$ places a restriction on the BVM parameter b . Since it is desirable to be able to quickly change System 32 to a static domain system by setting the growth parameter R equal to zero, the system’s parameters must satisfy the four static domain Turing conditions as well as the four growing domain Turing conditions in 30. Consider the first and third growing domain Turing conditions,

$$\begin{aligned} \omega (f_u + g_v) - 4R &< 0 \text{ and} \\ 2R (1 + D) - \omega (f_u + Dg_v) &< 0. \end{aligned}$$

Setting the growth rate $R = 0$ causes these conditions to simplify to the first and third static domain Turing conditions [11],

$$\begin{aligned} f_u + g_v &< 0 \text{ and} \\ f_u + Dg_v &> 0. \end{aligned} \tag{37} \tag{38}$$

Notice that Eqs. 37 and 38 imply that f_u, g_v must have opposite signs and $D \neq 1$ [11]. Since $D < 1$ for System 32, BVM kinetics parameters must be selected such that $f_u > 0$ and $g_v < 0$. Nondimensional BVM kinetics have partial derivatives

$$f_u = 1, \quad f_v = a, \quad g_u = h = \frac{2R}{\omega} - 1, \quad \text{and} \quad g_v = b,$$

where all partial derivatives have been evaluated at the unique steady state $(0, 0)$. Therefore, one must select $b < 0$ when choosing BVM parameter values for System 32.

Next, one must select values of ω, R, h, a, b (with $\omega, R > 0$ and $b < 0$) such that $(0, 0)$ is the only steady state of the system as discussed in Sect. 4.1. Finally, one must then select values of the remaining parameters C and D (with $D < 1$) such that the four mathematical Turing conditions in 30 are satisfied. Applying the conditions in 30 to System 32 gives

$$\left. \begin{aligned} \omega (1 + b) - 4R &< 0, \\ \omega^2 (a + b) - 2R\omega (1 + a + b) + 4R^2 &> 0, \\ 2R (1 + D) - \omega (1 + Db) &< 0, \text{ and} \\ \omega^2 (a + b) + R^2 (2 - \frac{1}{D} - D) & \\ + R\omega (\frac{1}{D} - b - 1 + Db - 2a) &< \frac{\omega^2}{4D} (1 + Db)^2. \end{aligned} \right\} \tag{39}$$

5 Application: Exponentially Growing Prolate Spheroid

To illustrate the effects of incorporating exponential growth into a Turing system, we implement System 4 on an exponentially growing prolate spheroidal domain. This extends previous research which analyzed a Turing system on a static prolate spheroidal domain [14].

5.1 Prolate Spheroid Domain

A prolate spheroid is obtained by rotating an ellipse around its major axis. Prolate spheroidal coordinates are defined by

$$\begin{aligned} x &= \frac{f}{2} \sqrt{(1 - \eta^2)(\xi^2 - 1)} \cos 2\pi\zeta, \\ y &= \frac{f}{2} \sqrt{(1 - \eta^2)(\xi^2 - 1)} \sin 2\pi\zeta, \\ z &= \frac{f}{2} \eta\xi, \end{aligned}$$

where ξ is the radial term with $\xi > 1$, $\eta = \cos \theta \in [-1, 1]$ where θ is the polar angle, $\zeta = \frac{\phi}{2\pi} \in [0, 1)$ where ϕ is the azimuthal angle, and f is the interfocal distance where $f = 2\sqrt{a^2 - b^2}$ and a, b are the semimajor and semiminor axes, respectively, of the ellipse [5]. The radial term ξ is inversely proportional to the prolate spheroid’s eccentricity E such that $E = \frac{1}{\xi}$. It then follows that fixing the value of ξ fixes the shape of the prolate spheroid. Prolate spheroids for differing values of f and ξ are depicted in Fig. 1; notice that increasing the value of ξ given a fixed value of f causes the spheroid to become more spherical in shape, while increasing the value of f given a fixed value of ξ increases the overall size of the spheroid without altering its shape [5].

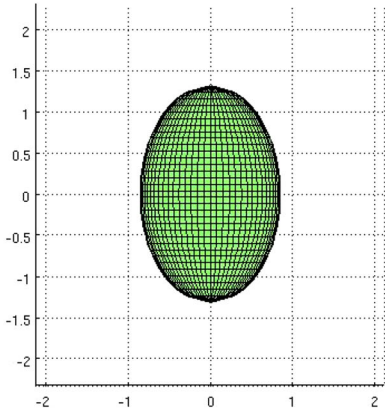
System 4 can represent a Turing system on an exponentially growing prolate spheroid simply by parameterizing the system with the proper position vector \mathbf{X} and by computing the Laplace–Beltrami operator Δ_s . We define the position vector \mathbf{X} on an exponentially growing prolate spheroid as

$$\mathbf{X}(\zeta, \eta, t) = \rho(t) \begin{pmatrix} \frac{f_0}{2} \sqrt{(\xi^2 - 1)(1 - \eta^2)} \cos 2\pi\zeta \\ \frac{f_0}{2} \sqrt{(\xi^2 - 1)(1 - \eta^2)} \sin 2\pi\zeta \\ \frac{f_0}{2} \xi \eta \end{pmatrix}, \tag{40}$$

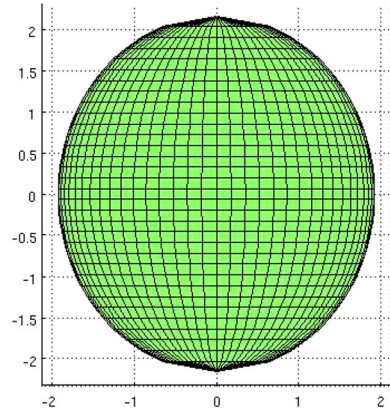
where $t \geq 0$, $\rho(t) = e^{Rt}$ is again the growth function with $R > 0$, and f_0 is the interfocal distance of the domain at $t = 0$. Parameterizing the prolate spheroid in this way gives isotropic growth.

Computing the Laplace–Beltrami operator Δ_s on an exponentially growing prolate spheroid requires $h_1 = |\mathbf{X}_\zeta|$ and $h_2 = |\mathbf{X}_\eta|$ from Eq. 3. It follows from Eq. 40 that

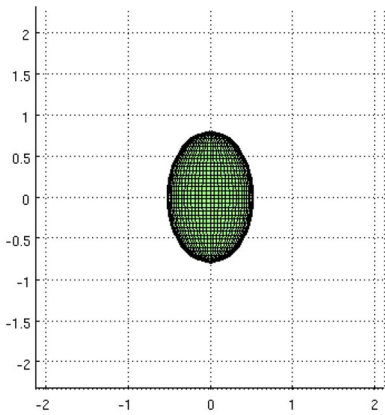
$$\mathbf{X}_\zeta = \rho(t) \begin{pmatrix} -\pi f_0 \sqrt{(\xi^2 - 1)(1 - \eta^2)} \sin(2\pi\zeta) \\ \pi f_0 \sqrt{(\xi^2 - 1)(1 - \eta^2)} \cos(2\pi\zeta) \\ 0 \end{pmatrix}$$



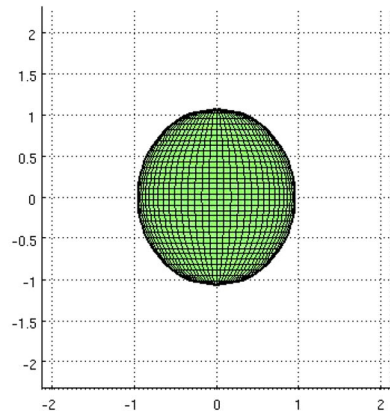
(a) $f = 2, \xi = 1.3141$, surface area = 4π



(b) $f = 2, \xi = 2.1640$, surface area = 16π



(c) $f = 1.2247, \xi = 1.3141$, surface area = 1.5π



(d) $f = 1, \xi = 2.1640$, surface area = 4π

Fig. 1 Prolate spheroids for different values of f and ξ

and

$$\mathbf{X}_\eta = \rho(t) \begin{pmatrix} -\frac{f_0}{2} \eta \sqrt{\frac{\xi^2-1}{1-\eta^2}} \cos 2\pi \zeta \\ -\frac{f_0}{2} \eta \sqrt{\frac{\xi^2-1}{1-\eta^2}} \sin 2\pi \zeta \\ \frac{f_0}{2} \xi \end{pmatrix}.$$

Thus

$$\begin{aligned} h_1 = |\mathbf{X}_\zeta| &= \sqrt{\mathbf{X}_\zeta \cdot \mathbf{X}_\zeta} = (\rho^2(t) \pi^2 f_0^2 (\xi^2 - 1) (1 - \eta^2))^{\frac{1}{2}} \\ &= \rho(t) \pi f_0 \sqrt{(\xi^2 - 1) (1 - \eta^2)}. \end{aligned} \tag{41}$$

Similarly,

$$h_2 = \rho(t) \frac{f_0}{2} \sqrt{\frac{\xi^2 - \eta^2}{1 - \eta^2}}. \tag{42}$$

It then follows that Eq. 3 becomes

$$\begin{aligned} \Delta_s = & \frac{1}{\pi^2 \rho^2 f_0^2 (1 - \eta^2) (\xi^2 - 1)} \phi_{\xi\xi} + \frac{4(1 - \eta^2)}{\rho^2 f_0^2 (\xi^2 - \eta^2)} \phi_{\eta\eta} \\ & - \frac{4\eta(2\xi^2 - \eta^2 - 1)}{\rho^2 f_0^2 (\xi^2 - \eta^2)^2} \phi_{\eta}. \end{aligned} \tag{43}$$

With the position vector defined in Eq. 40 and the Laplace–Beltrami operator defined in Eq. 43, System 4 now defines a Turing system on an exponentially growing prolate spheroid. Applying the linear stability analysis in Sect. 3 where the Y_k are prolate spheroidal harmonics [5] allows the Turing conditions in 30 to describe the Turing parameter space for the prolate spheroidal system. We select BVM kinetics for our growing prolate spheroidal system, so that System 32 along with Eqs. 40, 43 define a Turing system with BVM kinetics on an exponentially growing prolate spheroidal domain. This system shall be the system of interest for the remainder of the investigation.

5.2 Numerical Results

System 32 on an exponentially growing prolate spheroid was numerically implemented in Fortran using a forward time, central space finite difference scheme [10]. Parameter values for BVM kinetics and diffusion coefficient D were selected from the literature [2,9] and were as follows:

$$D = 0.516, \quad a = 1.112, \quad b = -1.01, \quad C = 0.$$

An initial interfocal distance of $f_0 = 2$ was selected and the radial term $\xi = 1.3141$ was fixed to give the initial domain a surface area of 4π , equivalent to the surface area of the unit sphere. Fixing the value of ξ also fixed the domain shape by fixing the eccentricity of the prolate spheroid. Simulations varied only in the growth rate parameter R and domain scale parameter ω , where R and ω were selected to satisfy the BVM Turing conditions in 39 as well as System 36 to ensure $(0, 0)$ was the only steady state of the system. Initial conditions for u and v consisted of random values $\phi \in [-0.5, 0.5]$ along the equator of the domain ($\eta = 0$) and zero elsewhere. Due to Turing systems’ characteristic sensitivity to initial conditions [17], the random values were seeded so that all simulations shared the same initial conditions.

We observed that the patterns produced by System 32 on an exponentially growing prolate spheroid continually evolve as time progresses; that is, the system does not converge to one final pattern (see Figs. 2, 3, 4). This observation of transient patterns is consistent with observations in the literature for a Turing system on other growing domains [12]. This contrasts with patterns created by static domain Turing systems in which the system converges to one final pattern [11]. Thus, the addition of growth to a Turing system causes a significant change in the system’s behavior.

We observed that the patterns produced by System 32 on an exponentially growing prolate spheroid often fluctuate between a striped pattern and a spotted pattern (see Fig. 2), though striped patterns were more prevalent due to our choice of BVM parameter C . We also observed

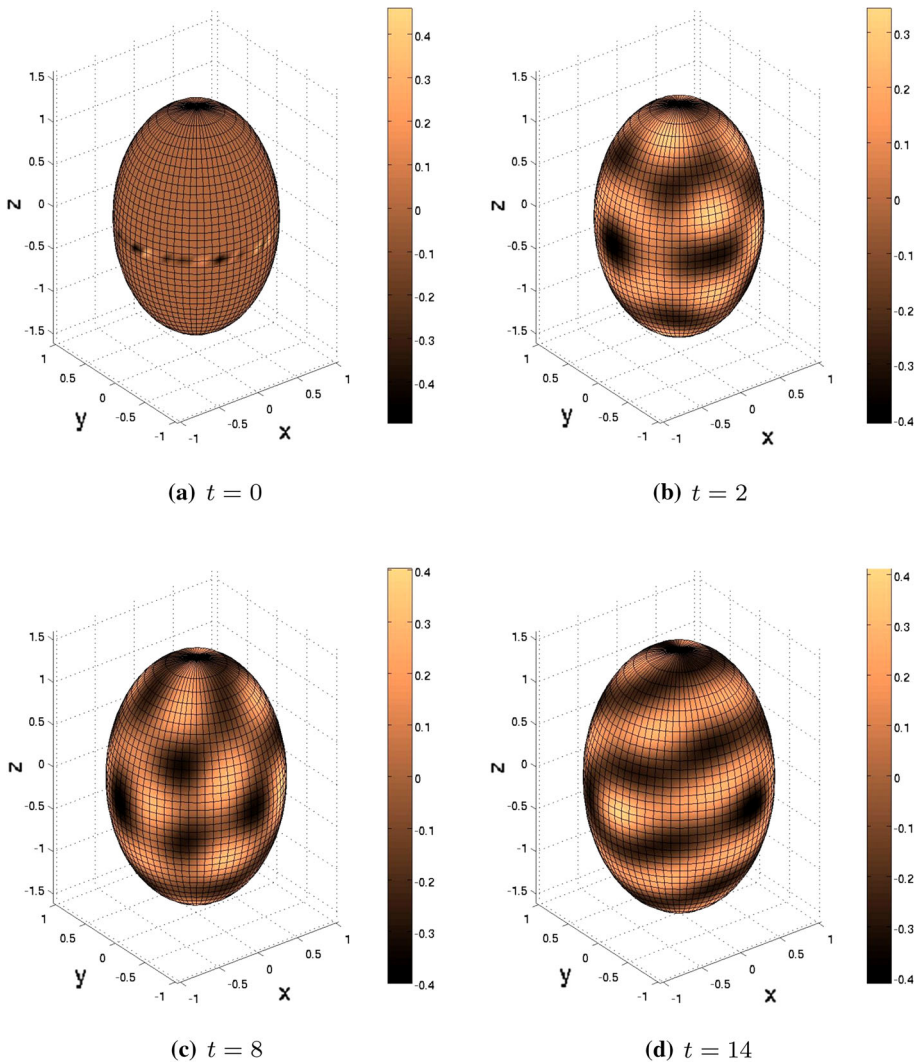


Fig. 2 Evolution of transient Turing patterns given by System 32 on a prolate spheroid with $f_0 = 2$, $\xi = 1.3141$, $R = 0.01$, and $\omega = 138.3$

that the patterns increase in complexity over time; that is, the number of spots/strips increases as elapsed time t progresses (see Fig. 3).

When varying the growth rate R , we observed that increasing R leads to more complex patterns (more stripes or more spots) at any given elapsed time of a simulation (compare Fig. 2 with Fig. 3). Increasing the domain scale parameter ω also yields more complex patterns at any given elapsed simulation time (compare Fig. 3 with 4). Another effect observed by increasing R or ω was a higher frequency of pattern change. In other words, the pattern evolves faster and changes from one pattern to another more quickly when a larger R or ω value is selected.

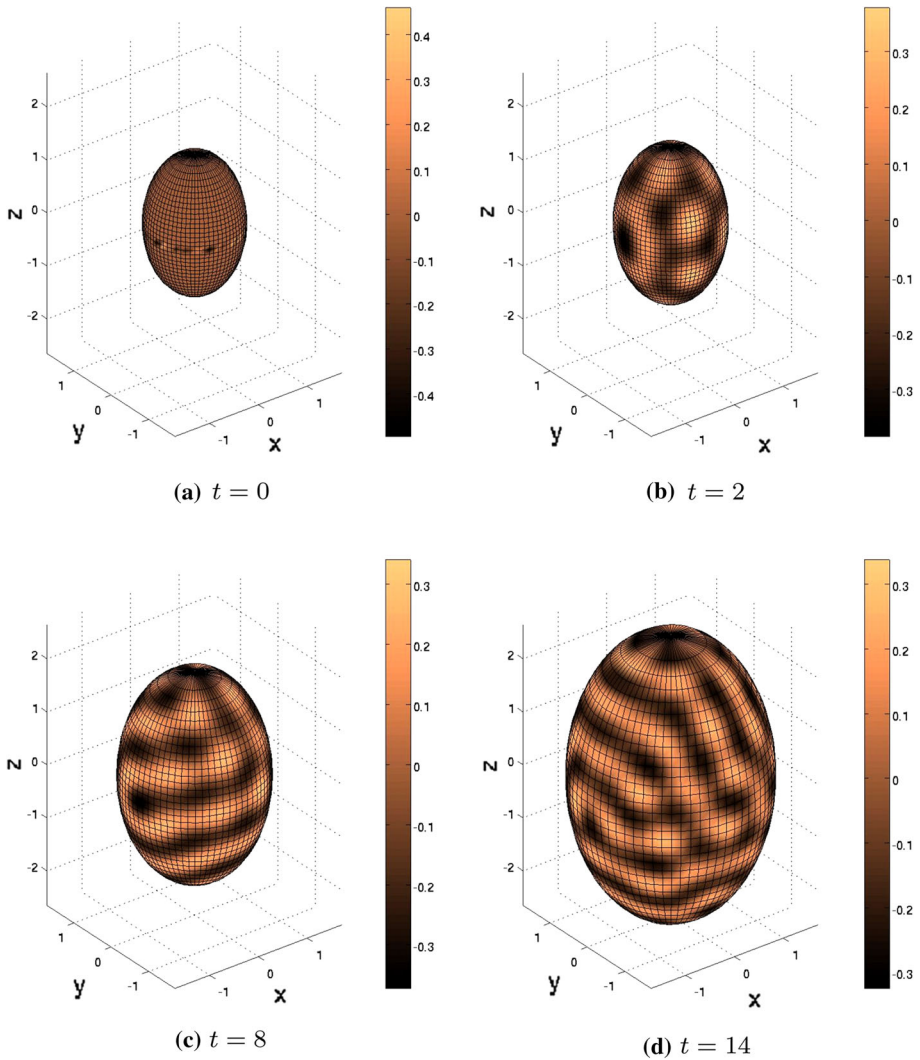


Fig. 3 Turing patterns given by System 32 on a prolate spheroid with $f_0 = 2, \xi = 1.3141, R = 0.05,$ and $\omega = 138.3.$ Observe that the the number of stripes/spots increases over time

6 Discussion

A strength of the exponentially growing domain Turing system in 4 is that it can be used to construct a Turing system on any of the eleven coordinate systems in which the Helmholtz equation is separable, such as the sphere [7]. This gives System 4 great flexibility and the potential to be used for mathematical modeling on a geometrically diverse group of domains. A further strength is that setting the growth rate to $R = 0$ completely reduces System 4 to the static domain Turing system [11],

$$\left. \begin{aligned} u_t &= D\nabla^2 u + \omega f(u, v), \\ v_t &= \nabla^2 v + \omega g(u, v). \end{aligned} \right\} \tag{44}$$

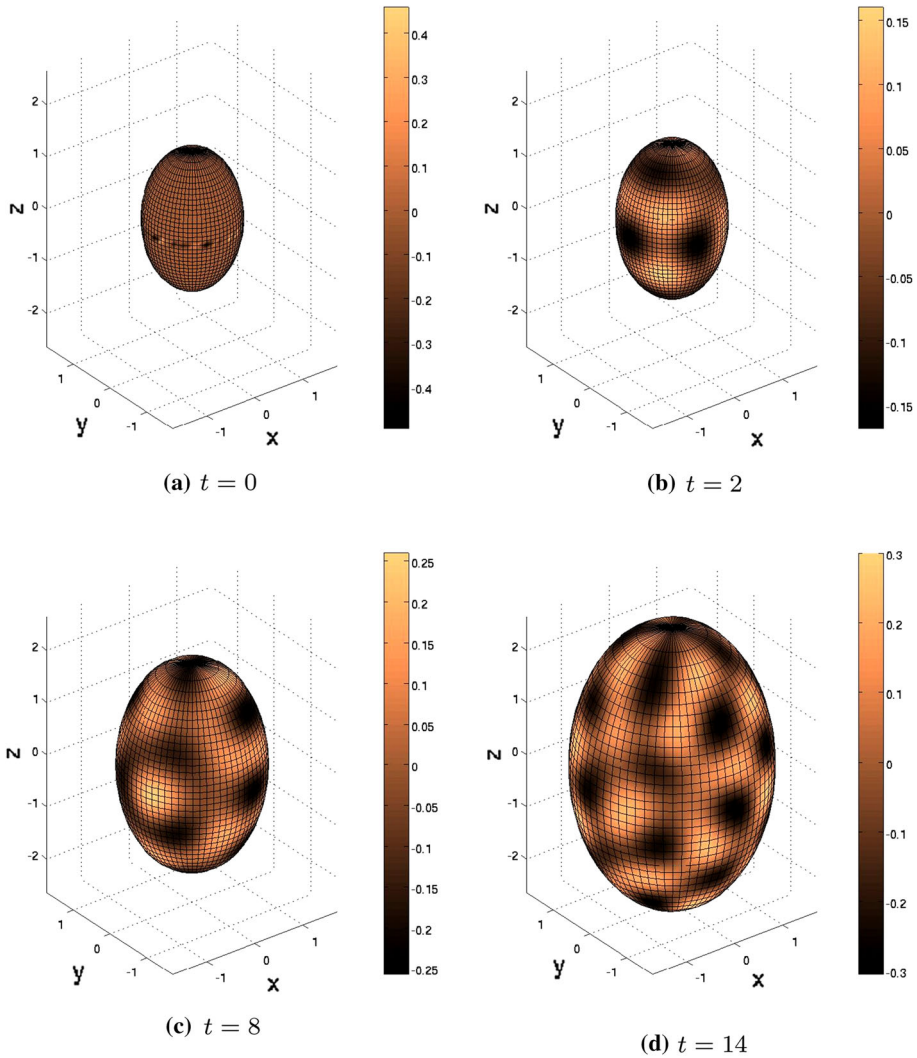


Fig. 4 Turing patterns given by System 32 on a prolate spheroid with $f_0 = 2$, $\xi = 1.3141$, $R = 0.05$, and $\omega = 69.15$. Notice how the patterns at each respective value of t are less complex compared to those in Fig. 3

Setting $R = 0$ reduces the four growing domain Turing conditions in 30 to the four static domain Turing conditions

$$\text{tr } A = f_u + g_v < 0, \tag{45a}$$

$$\det A = f_u g_v - f_v g_u > 0, \tag{45b}$$

$$f_u + Dg_v > 0, \tag{45c}$$

$$\det A < \frac{1}{4D} (f_u + Dg_v)^2, \tag{45d}$$

where all partial derivatives are evaluated at (u_0, v_0) and A is defined as in Eq. 14 [11]. Furthermore, if BVM kinetics are selected, setting $R = 0$ gives $h = -1$ (see Eq. 35), which

is the required h value needed to preserve the uniqueness of steady state $(0, 0)$ for static domain BVM Turing systems [2, 16].

Two important differences are noted when comparing the first two Turing conditions for the growing domain reaction–diffusion System 4 to those of System 44. Comparing Eqs. 18a to 45a shows that while the static case requires that the quantity $(f_u + g_v)$ be strictly negative, the growing case could allow for positive values of $(f_u + g_v)$ due to the $-4R$ term (recall that $\omega, R > 0$). This allows for the Turing parameter space of the growing domain System 4 to be larger than that of the static domain System 44. Furthermore, Eq. 18b implies

$$\omega^2 (f_u g_v - f_v g_u) > 2R [\omega (f_u + g_v) - 2R] > 2R [\omega (f_u + g_v) - 4R] = 2R \operatorname{tr} \tilde{A},$$

showing that for the growing domain System 4, the quantity $(f_u g_v - f_v g_u)$ need only be greater than some negative number (Eq. 18a requires that $\operatorname{tr} \tilde{A} < 0$). On the the other hand, the corresponding static domain Turing condition, given by Eq. 45b, again has a stricter requirement, forcing $(f_u g_v - f_v g_u)$ to be strictly positive. This again allows for the Turing parameter space of a growing domain system to be larger than that of a static domain system.

Numerical simulations of System 32 on an exponentially growing prolate spheroidal domain show that incorporating growth into a Turing system evokes an important change in the pattern-generating behavior of the system. Whereas static domain Turing systems converge to a final pattern as elapsed time t progresses, a growing domain Turing system generates transient patterns that continually evolve from one increasingly complex pattern to another. Furthermore, the overall complexity of the pattern produced by the system (number of stripes/spots) at a given t and the rate at which the transient patterns evolve can be moderated by altering certain system parameters. Increasing the growth rate R or the domain scale parameter ω not only increases the number of stripes/spots in the generated pattern at any given elapsed time t but also increases the rate of transient pattern evolution.

It would be interesting to compare the patterns produced by an exponentially growing Turing system on a prolate spheroidal domain with patterns generated by the system on other exponentially growing domains. It would also be interesting to see if similar results would be obtained by implementing other growth functions, such as linear or logistic growth, into the growing domain Turing system framework discussed in Sect. 2. We expect growth rate and domain scale to play critical roles in other domains as well.

References

1. Barrio, R.: Turing systems: a general model for complex patterns in nature. *Electron J. Theor. Phys.* **4**(15), 1–26 (2007)
2. Barrio, R., Baker, R., Vaughan, B., Tribuzy, K., de Carvalho, M., Bassanezi, R., Maini, P.: Modeling the skin pattern of fishes. *Phys. Rev. E* **79**(3), 031,908–1–031,908–11 (2009)
3. Barrio, R., Varea, C., Aragon, J., Maini, P.: A two-dimensional numerical study of spatial pattern formation in interacting turing systems. *B Math. Biol.* **61**(3), 483–505 (1999)
4. Ermentrout, B.: Stripes or spots? Nonlinear effects in bifurcation of reaction–diffusion equations on the square. *Proc. R. Soc. Lond. A Math.* **434**(1891), 413–417 (1991)
5. Flammer, K.: *Spheroidal Wave Functions*. Stanford University Press, Palo Alto (1957)
6. Gierer, A., Meinhardt, H.: A theory of biological pattern formation. *Kybernetik* **12**, 30–39 (1972)
7. Gjorgjieva, J., Jacobsen, J.: Turing patterns on growing spheres: the exponential case. *Discrete Cont. Dyn. Syst. Suppl.* **2007**, 436–445 (2007)
8. Leppänen, T.: Computational studies of pattern formation in turing systems. Ph.D. thesis, Helsinki University of Technology (2004)
9. Leppänen, T., Karttunen, M., Barrio, R., Kaski, K.: Morphological transitions and bistability in turing systems. *Phys. Rev. E* **70**, 066,202 (2004). doi:[10.1103/PhysRevE.70.066202](https://doi.org/10.1103/PhysRevE.70.066202)

10. Morton, K., Mayers, D.: Numerical Solution of Partial Differential Equations: an Introduction, 2nd edn. Cambridge University Press, Cambridge (2005)
11. Murray, J.: Mathematical Biology II, 3rd edn. Springer, New York (2003)
12. Plaza, R., Sanchez-Garduno, F., Padilla, P., Barrio, R., Maini, P.: The effect of growth and curvature on pattern formation. *J. Dyn. Differ. Equ.* **16**(4), 1093–1121 (2004)
13. Sick, S., Reinker, S., Timmer, J., Schlake, T.: Hair follicle spacing through a reaction-diffusion mechanism. *Science* **314**, 1447–1450 (2006)
14. Striegel, D., Hurdal, M.: Chemically based mathematical model for development of cerebral cortical folding patterns. *PLoS Comput. Biol.* **5**(9), e1000524 (2009)
15. Turing, A.: The chemical basis of morphogenesis. *Philos. Trans. R. Soc. B* **237**, 37–72 (1952)
16. Varea, C., Hernandez, D., Barrio, R.: Soliton behaviour in a bistable reaction diffusion model. *J. Math. Biol.* **54**, 797–813 (2007)
17. Venkataraman, C., Sekimura, T., Gaffney, E., Maini, P., Madzvamuse, A.: Modeling parr-mark pattern formation during the early development of Amago trout. *Phys. Rev. E* **84**, 041,923 (2011). doi:[10.1103/PhysRevE.84.041923](https://doi.org/10.1103/PhysRevE.84.041923)
18. Zwillinger, D.: Handbook of Differential Equations. Academic Press, San Diego (1989)